Ab Initio and Density Functional Theory Study of the Geometry and Reactivity of Benzyne, 3-Fluorobenzyne, 4-Fluorobenzyne, and 4,5-Didehydropyrimidine

Wilfried Langenaeker, Frank De Proft, and Paul Geerlings*

Eenheid Algemene Chemie, Vrije Universiteit Brussel, Faculteit Wetenschappen, Pleinlaan 2, B-1050 Brussel, Belgium

Received: January 7, 1998; In Final Form: April 1, 1998

The geometries and reactivity of three intermediates of the aromatic nucleophilic substitution, 3-fluorobenzyne, 4-fluorobenzyne, and 4,5-didehydropyrimidine, are studied using ab initio molecular orbital theory and density functional theory (DFT). As compared to the traditional ab initio methods, all DFT methods clearly assign more triple-bond character to the carbon−carbon bond in the ring on which the addition occurs. Furthermore DFT methods are found to correctly describe reactive intermediates in which electron correlation effects are expected to be large. The reactivity of the three intermediates is studied using the chemical concepts of electronegativity and hardness. The Fukui function was calculated for a nucleophilic attack at different DFT levels and found to be an adequate reactivity descriptor.

1. Introduction

"Identification of the intermediates in a multistep reaction is a major objective of studies of reaction mechanisms. When the nature of each intermediate is fairly well understood, a great deal is known about the reaction mechanism."[1] Present day quantum chemical methods offer a useful alternative to experimental techniques when studying the characteristics of these intermediates. This principle is used to study intermediates in the aromatic nucleophilic substitution.[2−4] The two main mechanistic forms of aromatic nucleophilic substitution are the unimolecular (S_N1) mechanism and the bimolecular (S_N2) mechanism. The former mechanism involves a rate-limiting heterolysis of the bond to the displaced group followed by reaction with the nucleophile. The second mechanism involves both bonding by the nucleophile and heterolysis of the bond to the displaced group in forming the transition state of the rate-limiting step. The great majority of aromatic nucleophilic substitution reactions follow the S_N2 mechanism in the form of an addition−elimination reaction. The form of an elimination−addition S_N2 (Figure 1), known as the benzyne mechanism, is less common. In this mechanism a triple bond is formed in the elimination step. The most commonly held view concerning the nature of this bond is that two sp^2 electrons on neighboring carbons occupy an orbital formed by the overlap of sp^2 orbitals, giving rise to the third localized bond. Our attention is focused on the addition reaction in the second step of this mechanism (Figure 1), i.e., the theoretical study of the reaction of a nucleophile with the triple bond in unsymmetrically substituted benzynes (e.g., *o*-didehydrobenzene or *o*-benzyne). The systems considered are 3- and 4-fluorobenzynes and 4,5-didehydropyrimidine. The reason for interest in these systems is twofold. First of all, from the *structural* point of view, the presence of a triple bond in both the benzynes and the hetarynes provides a challenge at the calculational level. As one expects the role of electronic correlation effects to be fairly large in a system with high local concentrations of electrons, the calculational methods used to treat these effects may have a considerable influence. In wave function theory the presence of electron correlation calls for a post-Hartree−Fock level of calculation. The most widely used are Møller−Plesset (MP) perturbation theory,[5] configuration interaction (CI) methods,[6] the generalized valence bond (GVB) method,[7,8] coupled cluster (CC) methods,[9] and multiconfigurational self-consistent field (MCSCF) theory.[10] Most of these techniques are however very expensive (i.e., require large CPU time and state of the art hardware)[11] and not applicable for large systems in combination with large basis sets. Even though the use of the latter methods in a reduced form is possible,[12] a very attractive alternative can be found in density functional theory (DFT) methods.[13]

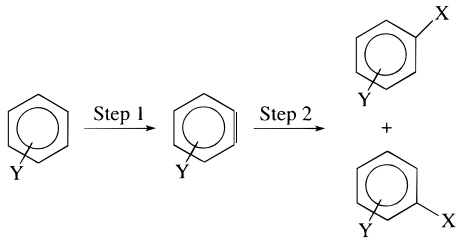

Figure 1. Elimination−addition or benzyne mechanism for the aromatic nucleophilic substitution.

These methods are based on the Hohenberg−Kohn theorems,[14] according to which the electron density $\rho(r)$ can be used as the fundamental variable determining all atomic and molecular properties. DFT automatically incorporates electron correlation via the exchange−correlation functional,[13] and practical calulations can be performed using the Kohn−Sham method.[15] Furthermore, algorithms are being developed to solve the Kohn−Sham equations, scaling linearly with the number of basis functions.[16] In a first part of this paper, the use of different DFT methods in combination with different basis sets in the geometry optimizations is investigated.

A second reason we are interested in these systems is the fact that the study of *reactions* involving exotic reaction partners such as these reactive intermediates is interesting per se. In the case of the hetaryne, the first clear-cut experimental evidence that 4,5-didehydropyrimidine should undergo preferential nucleophilic attack at the 4- rather than the 5-position was given

* To whom all correspondence should be sent. E-mail address: pgeerlin@vub.ac.be.

S1089-5639(98)00706-3 CCC: $15.00
Published on Web 06/25/1998

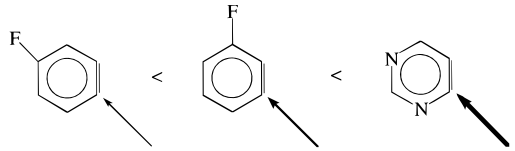

Figure 2. Regioselectivity for a nucleophilic attack in the 3- and 4-fluorobenzynes and the 4,5-didehydropyrimidine.

by Promel et al.[17] in 1992. In their investigation of the reactivity of the 2-*tert*-butyl-4,5-didehydropyrimidine toward ethanol only 4-ethoxy-2-*tert*-butylpyrimidine was isolated in significant amounts. This clearly demonstrates the preference of a nucleophilic attack at the 4-position (Figure 2). In comparison with the substituted benzynes a higher regioselectivity was found (meta/ortho ratio varying from 16:1 to 100:1 for 3-fluorobenzyne,[18] para/meta ratio varying from 1:1 to 2:1 for 4-fluorobenzyne[18] and the absence of a 5-substituted product for the hetarynes[17]), yielding the following general regioselectivity sequence:

4-fluorobenzyne < 3-fluorobenzyne <
2-*tert*-butyl-4,5-didehydropyrimidine

This suggests an increasing dissymmetry in the triple bond. Schematically the regioselectivity in the three systems considered can be depicted as is done in Figure 2. This sequence was previously investigated using the molecular electrostatic potential (MEP)[19] with moderate wave function techniques. Also some preliminary results of a reactivity study using Pearson's hard and soft acids and bases (HSAB) principle[20] were reported. This principle states that hard acids prefer to react with hard bases, whereas soft acids prefer to react with soft bases. The Fukui function,[21] frequently used[22] among others by the present authors[23] as a reactivity descriptor for soft−soft interactions,[22,23] was calculated for the hetaryne. The second part of this paper will deal with the results of a reactivity study based on straightforward considerations using the effect of the substituents and heteroatoms on the electron density distribution and using the Fukui function f^+ in its condensed form calculated at different DFT levels.

2. Theory and Computational Details

Density functional theory provides a natural framework for a quantitative description of chemical reactivity. Long-known concepts readily used by chemists such as electronegativity, hardness and softness, and frontier molecular orbital treatments of reactivity all emerge naturally from this theory. Furthermore, theoretical justification was provided for the Sanderson electronegativity equalization principle[24] and Pearson's HSAB and maximum hardness principle. Within density functional theory global softness, S, can be defined[25] as the inverse of the global hardness η:[26]

$$S = \frac{1}{2\eta} = \left(\frac{\partial N}{\partial \mu}\right)_{v(r)} \tag{1}$$

where μ is the electronic chemical potential,[27] which was also identified with the negative of the electronegativity, χ.[13]

$$\mu = \left(\frac{\partial E}{\partial N}\right)_{v(r)} = -\chi \tag{2}$$

and E denotes the energy, N the number of electrons of the system, and $v(r)$ the external potential. Based on eq 1 and the fact that the local quantity should intergrate to the global softness

$$S = \int s(r)\, dr \tag{3}$$

local softness $s(r)$ can be identified with

$$s(r) = \left(\frac{\partial \rho}{\partial N}\right)_{v(r)}\left(\frac{\partial N}{\partial \mu}\right)_{v(r)} \tag{4}$$

This local quantity can be used to describe intermolecular as well as intramolecular reactivity sequences. The first derivative in eq 4 is the Fukui function, $f(r)$, the intramolecular reactivity index for an N-electron system defined by Parr and Yang.[21] Due to the discontinuity in this derivative at the N-value considered, different intramolecular reactivity indices[21] can be defined based on eq 4. In a finite difference approximation, these indices can be written as

$$f^-(r) = \rho_N(r) - \rho_{N-1}(r) \tag{5}$$

in the case of an electrophilic attack, and

$$f^+(r) = \rho_{N+1}(r) - \rho_N(r) \tag{6}$$

in the case of a nucleophilic attack.

$\rho_M(r)$ is the electron-density function of the atomic or molecular anion ($M = N + 1$) or cation ($M = N - 1$), calculated at the geometry of the neutral system ($M = N$).

In a "condensed" version these indices[28] are

$$f_k^- = q_k(N) - q_k(N-1) \tag{7}$$

$$f_k^+ = q_k(N+1) - q_k(N) \tag{8}$$

where $q_k(N)$, $q_k(N+1)$, and $q_k(N-1)$ are the atomic electron population[28] at the atom k for the N-, $(N+1)$- and $(N-1)$-electron system.

The electron densities needed to evaluate the condensed Fukui functions were obtained within a density functional framework using three types of exchange−correlation functionals:

·The local density approximation (LDA), combining the Dirac expression[29] for exchange with Vosko, Wilk, and Nusair's expression for the correlation energy of a homogeneous electron gas;[30]

·The BLYP functional, a combination of Becke's gradient-corrected exchange functional[31] with Lee, Yang, and Parr's correlation functional;[32]

·Becke's three-parameter functional B3PW91 and the B3LYP functional.[33]

All calculations were performed using the Gaussian 94 package[34] running on a Cray J916/8-1024 of the Brussels Free Universities Computer center. All DFT calculations were performed using Dunning's correlation consistent cc-pVDZ and cc-pVTZ, being [3s2p1d/2s1p] and [4s3p2d1f/3s2p1d] contractions of (9s4p1d/4s1p) and (10s5p2d1f/5s2p1d) primitive sets, respectively,[35] which, among others in our own work, turned out to yield excellent results in the calculation of atomic charges, dipole moments, IR intensities, electrostatic potentials, Fukui functions, ionization energies, electron affinities, electronegativities, and hardnesses.[36] The geometries were fully optimized at all levels using these basis sets. At the cc-pVDZ level, additional MP2 and QCISD[37] calculations were performed to serve as a reference. All geometries are available from the authors upon request.

Atomic populations were calculated using the orbital-based natural population analysis method (NPA),[38] which can be obtained accurately using DFT methods.[36b,39]

3. Results and Discussions

3.1. Geometries. In the past, a vast number of studies concerning the geometry and the energetics of the *o*-, *m*-, and

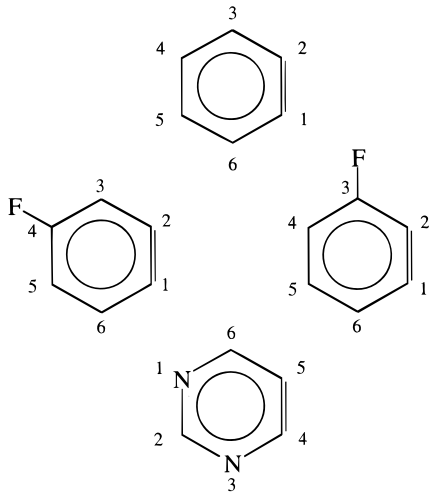

Figure 3. Geometry and numbering of the ring atoms in *o*-benzyne, 3-fluorobenzyne, 4-fluorobenzyne, and 4,5-didehydropyrimidine.

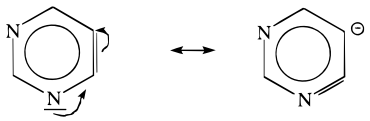

Figure 4. σ delocalization of the nitrogen free electron pair in 4,5-didehydropyrimidine.

p-benzynes[40] have been performed. However, almost all of these studies were conducted using molecular orbital theory, and very few DFT results were publised until now (see, for example, ref 40p). In this part, the geometry of the *o*-benzyne, 3-F-benzyne, 4-F-benzyne, and the 4,5-didehydropyrimidine will be assessed and discussed. The structures of these compounds can be found in Figure 3 together with the numbering of the different atoms. The structural parameters of *o*-benzyne are listed in Table 1. In addition to the performed DFT, MP2, and QCISD calculations, the results from geometry optimization of Kraka and Cremer[40l] (CCSD(T)/6-31G(d,p) and MP2/6-31G-(d,p)) and Lindh et al.[40n] (CASSCF(8,8) with the DZP and 5s4p2d/3s2p basis sets) are given. Concentrating on the 6-31G-(d,p) basis set, it can be seen that the BLYP functional and the MP2 method generate a triple-bond distance in best agreement with the CCSD(T) result. All DFT methods predict this bond to be less than 1.26 Å, thus assigning more triple-bond character to this species (vide infra). However, bond lengths of 1.262 and 1.251 Å are observed when multireference character is introduced in the calculations by means of the CASSCF(8,8) calculations. It should also be noted that the subtle prediction that the C_3-H bond length is shorter than the C_4-H bond length is reproduced by all DFT methods, except the BLYP functional. At the cc-pVDZ level, the bond lengths of the triple bond become somewhat larger; they are however still below 1.26 Å for the exact exchange functionals B3LYP and B3PW91. Surprisingly, the MP2 bond is lengthend by more than 0.01 Å, so that the agreement with the QCISD calculated bond length disappears. At the cc-pVTZ level, a further drop of the triple-bond length is witnessed.

Table 2 lists the geometrical parameters of the 3-F-benzyne, 4-F-benzyne, and the 4,5-didehydropyrimidine. As can be noticed from this table, the triple bond in 3-F-benzyne is somewhat shorter than the triple bond in benzyne, whereas the triple-bond length in 4-F-benzyne is somewhat larger. A simple explanation can be provided by considering the charges of the two carbon atoms in the triple bond; in benzyne, the B3PW91/cc-pVTZ sum of the charges of these two carbon atoms is 11.961, in 3-F-benzyne, it is 11.984, and in 4-F-benzyne, it is 11.947. As can be seen, the triple-bond carbons carry the largest number of electrons in 3-F-benzyne, followed by benzyne and 4-F-benzyne. One can expect that a larger number of electrons on the bond atoms will increase the bond length; this explains the calculated sequence of triple-bond lengths. It has to be remarked that this is not solely a σ effect, since the σ populations on the carbon atoms are 10.065 (benzyne), 10.029 (3-F-benzyne), and 9.999 (4-F-benzyne). Again for the two fluorobenzynes, the BLYP functional predicts the bond lengths in closest agreement with the QCISD results, being an approximation to the CCSD value. Going from the cc-pVDZ to the cc-pVTZ again shortens the bond lengths substantially. For the exact exchange levels B3LYP and B3PW91, bond lengths close to 1.24 Å are predicted, implying substantial domination of triple-bond character (the experimental bond length of the carbon−carbon double bond in acetylene is 1.203 Å, whereas the carbon−carbon bond in ethylene is 1.339 Å, averaging to 1.271 Å).

Concentrating on the 4,5-didehydropyrimidine, the bonds between C_4 and C_5 and between N_3 and C_4 both have triple bond character, the shortest bond at all levels being the nitrogen−carbon bond. This can be explained by a σ conjugation effect of the nitrogen atom, as was already recognized by Radom et al.[40a]

This σ-conjugation effect, shown in Figure 4, will also be of utmost importance when the reactivity of this molecule toward a nucleophilic attack is discussed. At the MP2 level, the C_4-C_5 bond length is now in agreement with the exact exchange results, but the N_3-C_4 bond distance is again overestimated. The cc-pVTZ basis set again lowers all DFT calculated bond lengths.

Finally, comparing all bond lengths at the cc-pVDZ level with the QCISD results yields a mean absolute deviation of 0.012 Å for the LDA method, BLYP and B3LYP both deviate 0.007 Å, and B3PW91 deviates 0.009 Å. For the MP2 level, the deviation is the smallest, being only 0.005 Å. For the angles however, LDA deviates 1.14°, BLYP 1.1°, B3LYP 0.6°, and B3PW91 1.0°. With 3.4, MP2 clearly does worse in predicting the bond angles of these systems as compared with DFT.

From this part of our study, it can be concluded that density functional calculation methods beyond the local density approximation level clearly offer the ability to study these reactive intermediates in which electron correlation effects can be expected to have a large influence on the results. All DFT methods seem to assign more triple-bond character to the carbon−carbon bond where the hydrogens were abstracted as compared with the single-reference electron correlation methods.

3.2. Reactivity. As mentioned in the Introduction, our main concern is the study of the regioselectivity in the second step of the aromatic nucleophilic substitution reaction following the elimination−addition mechanism of the S_N2-type reaction. First we will consider the reactivity of the two fluorobenzynes. One usually assumes that in the addition step the nucleophilic attack takes place at the point of least electron density. In determining this point, two effects of the F-substitution have to be considered: the inductive and the resonance effect.

When considering the resonance effect, the relevant resonance forms for the two substituted benzynes are depicted in Figure 5.

On the basis of this resonance effect, it clear that in the case of 4-fluorobenzyne a reversed polarization of the triple bond is expected, in contrast to the case of 3-fluorobenzyne. This is confirmed by the total electronic NPA populations, obtained at

TABLE 1: Calculated Geometrical Parameters (distances *R* in Angstroms and Angles *A* in Degrees) of *o*-Benzyne at the Four DFT Levels and with the 6-31G(d,p), cc-pVDZ, and cc-pVTZ Basis Sets. Also Listed Are Reference MP2 and QCISD Calculations, Together with Recent MP2,[40l] CCSD(T),[40l] and CASSCF(8,8)[40n] Literature Results

level	basis set	R_{C1C2}	R_{C2C3}	R_{C3C4}	R_{C4C5}	R_{C2H}	R_{C3H}	A_{C6C1C2}	A_{C2C3C4}	A_{C6C5C4}
LDA	6-31G(d,p)	1.257	1.375	1.397	1.409	1.095	1.097	127.2	110.1	122.3
BLYP		1.264	1.393	1.425	1.414	1.092	1.092	127.0	110.5	122.4
B3LYP		1.251	1.385	1.413	1.407	1.085	1.087	127.1	110.4	122.5
B3PW91		1.251	1.382	1.411	1.404	1.085	1.088	127.2	110.2	122.6
MP2		1.268	1.389	1.405	1.410	1.080	1.083	126.6	111.2	122.6
CCSD(T)		1.269	1.394	1.411	1.413	1.081	1.084	126.4	111.2	122.4
LDA	cc-pVDZ	1.260	1.379	1.411	1.399	1.101	1.103	127.2	110.0	122.8
BLYP		1.267	1.397	1.420	1.427	1.098	1.101	127.1	110.4	122.5
B3LYP		1.255	1.388	1.415	1.409	1.091	1.094	127.2	110.3	122.6
B3PW91		1.254	1.384	1.413	1.405	1.091	1.094	127.3	110.1	122.7
MP2		1.280	1.401	1.417	1.420	1.094	1.097	126.6	110.6	122.4
QCISD		1.268	1.402	1.415	1.422	1.094	1.097	126.7	110.7	122.5
LDA	cc-pVTZ	1.245	1.369	1.402	1.390	1.091	1.094	127.3	110.0	122.7
BLYP		1.253	1.387	1.419	1.408	1.086	1.090	127.2	110.4	122.4
B3LYP		1.241	1.379	1.407	1.401	1.080	1.083	127.3	110.3	122.6
B3PW91		1.242	1.376	1.406	1.398	1.081	1.085	127.4	110.0	122.6
CASSCF(8,8)	DZP	1.262	1.406	1.397	1.426	1.075	1.078			
	(5s4p2d/3s2p)	1.251	1.399	1.390	1.420	1.070	1.073			

TABLE 2: Calculated Geometrical Parameters (Distances *R* in Angstroms and Angles *A* in Degrees) of 3-Fluorobenzyne (First Series), 4-Fluorobenzyne (Second Series), and 4,5-Didehydropyrimidine (Third Series) at the Four DFT Levels and the MP2 and QCISD Level with the cc-pVDZ and cc-pVTZ Basis Sets

	LDA		BLYP		B3LYP		B3PW91		MP2	QCISD
	cc-pVDZ	cc-pVTZ	cc-PVDZ	cc-pVTZ	cc-PVDZ	cc-pVTZ	cc-PVDZ	cc-pVTZ	cc-PVDZ	cc-PVDZ
R_{C1C2}	1.262	1.249	1.270	1.256	1.258	1.245	1.257	1.245	1.279	1.270
R_{C2C3}	1.381	1.371	1.396	1.385	1.387	1.378	1.385	1.376	1.394	1.398
R_{C3C4}	1.406	1.397	1.421	1.412	1.408	1.401	1.407	1.400	1.410	1.408
R_{C4C5}	1.395	1.386	1.413	1.405	1.405	1.398	1.402	1.395	1.417	1.420
R_{C5C6}	1.414	1.406	1.430	1.422	1.418	1.410	1.416	1.409	1.417	1.417
R_{C6C1}	1.367	1.357	1.385	1.375	1.376	1.366	1.372	1.363	1.397	1.394
R_{C3F}	1.325	1.323	1.357	1.357	1.341	1.338	1.335	1.332	1.338	1.341
A_{C6C1C2}	135.2	135.0	134.6	134.4	135.3	135.1	135.9	135.8	129.9	133.4
A_{C1C2C3}	118.1	118.3	118.2	118.6	117.8	118.1	117.5	117.6	122.4	118.9
R_{C1C2}	1.258	1.244	1.265	1.251	1.253	1.239	1.252	1.240	1.278	1.267
R_{C2C3}	1.377	1.367	1.395	1.387	1.387	1.379	1.383	1.375	1.397	1.402
R_{C3C4}	1.407	1.399	1.422	1.413	1.409	1.401	1.408	1.401	1.411	1.408
R_{C4C5}	1.403	1.394	1.419	1.411	1.411	1.403	1.408	1.401	1.421	1.422
R_{C5C6}	1.403	1.395	1.419	1.411	1.407	1.400	1.405	1.398	1.409	1.409
R_{C6C1}	1.381	1.372	1.399	1.390	1.390	1.381	1.386	1.379	1.406	1.405
R_{C4F}	1.334	1.333	1.367	1.367	1.351	1.349	1.346	1.343	1.352	1.351
A_{C6C1C2}	127.9	127.8	127.7	127.9	128.0	128.1	127.9	127.9	125.6	127.0
A_{C1C2C3}	127.0	127.3	126.8	126.9	126.8	126.9	127.1	127.9	127.9	126.7
R_{C4C5}	1.285	1.270	1.295	1.281	1.284	1.270	1.284	1.272	1.285	1.296
R_{C5C6}	1.419	1.408	1.437	1.426	1.432	1.421	1.431	1.421	1.416	1.436
R_{C6N1}	1.343	1.337	1.365	1.360	1.354	1.348	1.341	1.345	1.362	1.358
R_{N1C2}	1.313	1.305	1.328	1.320	1.319	1.312	1.317	1.310	1.33	1.332
R_{C2N3}	1.387	1.381	1.417	1.411	1.397	1.392	1.392	1.388	1.407	1.394
$^{R}_{N3C4}$	1.264	1.255	1.277	1.268	1.263	1.255	1.261	1.253	1.293	1.280
A_{C3C4C5}	144.6	144.1	145.2	144.7	147.6	146.0	148.4	148.2	141.6	147.8
A_{C4C5C6}	105.4	106.3	105.4	106.2	102.9	103.8	102.0	102.6	110.8	102.9

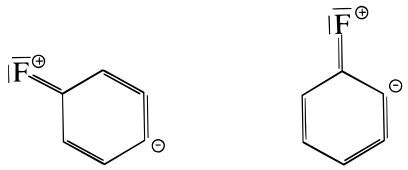

Figure 5. Relevant resonance structures of 3- and 4-fluorobenzyne.

different levels of calculation using different basis sets, given in Table 3. It is seen that for 3-fluorobenzyne in all cases the population on the C_1 atom is smaller than the population on the C_2 atom, whereas for 4-fluorobenzyne the opposite is found, leading to the wrong regioselectivity for a nucleophilic attack. This is however not a problem if one takes into account that the third bond on which the reaction takes place in these benzynes is located in the σ plane. Using this information, one can propose to look at the electronic population on the C atoms in terms of a σ and a π contribution. These different contributions can be obtained by investigating the contributions per atomic orbital to the total population. On the basis of the orientation of these orbitals, one can make the following distinction: orbitals perpendicular to the molecular plane are describing the π system; orbitals in the molecular plane are describing the σ system. Considering only the σ populations on the different C atoms leads to the correct polarization of the triple bond in both the 3-fluorobenzyne and 4-fluorobenzyne. Furthermore it is seen that the σ population on C_1 is less than 5, 5 being the expected σ population for a nonpolarized bond (6 minus 1 π electron), possibly indicating the actual occurrence of a nucleophilic attack.

The main question now is whether this polarization of the third (σ) bond can be explained in terms of the inductive effect of the fluoro atom. The σ populations on both carbons, C_1 and

TABLE 3: Calculated NPA Electron Populations (in au) of 3-Fluorobenzyne, 4-Fluorobenzyne, and 4,5-Didehydropyrimidine at the Four DFT Levels with the cc-pVDZ and cc-pVTZ Basis Sets

			NPA(tot)		NPA(π)		NPA(σ)	
system	level	basis set	C_1	C_2	C_1	C_2	C_1	C_2
3-fluorobenzyne	SVWN	cc-pVDZ	5.885 36	6.092 51	0.986 36	0.964 79	4.899 00	5.127 72
	BLYP		5.890 16	6.092 81	0.986 76	0.960 01	4.903 40	5.132 80
	B3LYP		5.877 46	6.107 44	0.992 16	0.959 14	4.885 30	5.148 30
	B3PW91		5.875 13	6.112 54	0.992 55	0.960 03	4.882 58	5.152 51
	SVWN	cc-pVTZ	5.871 49	6.099 25	0.985 89	0.966 53	4.885 60	5.132 72
	BLYP		5.876 85	6.099 92	0.986 74	0.962 62	4.890 11	5.137 30
	B3LYP		5.863 58	6.116 53	0.991 77	0.962 55	4.871 81	5.153 98
	B3PW91		5.860 04	6.123 52	0.992 16	0.962 84	4.867 88	5.160 68
4-fluorobenzyne	SVWN	cc-pVDZ	5.971 54	5.966 96	0.989 08	0.955 17	4.982 46	5.011 79
	BLYP		5.975 57	5.972 22	0.986 12	0.952 35	4.989 45	5.019 87
	B3LYP		5.977 27	5.974 42	0.992 04	0.951 82	4.985 23	5.022 60
	B3PW91		5.979 79	5.973 96	0.992 43	0.953 59	4.987 36	5.020 37
	SVWN	cc-pVTZ	5.970 30	5.960 40	0.988 66	0.956 46	4.981 64	5.003 94
	BLYP		5.973 02	5.967 95	0.987 13	0.953 73	4.985 89	5.014 22
	B3LYP		5.975 25	5.969 94	0.993 23	0.953 25	4.982 02	5.016 69
	B3PW91		5.978 56	5.968 55	0.993 17	0.954 96	4.985 39	5.013 59

system	level	basis set	C_4	C_5	C_4	C_5	C_4	C_5
4,5-didehydropyrimidine	SVWN	cc-pVDZ	5.628 44	6.202 76	0.919 86	0.848 13	4.708 58	5.354 63
	BLYP		5.619 96	6.211 00	0.921 90	0.842 24	4.698 06	5.368 76
	B3LYP		5.576 03	6.241 78	0.937 56	0.838 96	4.638 47	5.402 82
	B3PW91		5.572 61	6.247 48	0.937 09	0.838 62	4.635 52	5.408 86
	SVWN	cc-pVTZ	5.668 21	6.190 99	0.916 11	0.855 64	4.752 10	5.335 35
	BLYP		5.655 95	6.202 03	0.916 46	0.851 44	4.739 49	5.350 59
	B3LYP		5.610 84	6.235 89	0.931 77	0.849 43	4.679 07	5.386 46
	B3PW91		5.609 57	6.241 42	0.933 53	0.846 81	4.676 04	5.394 61

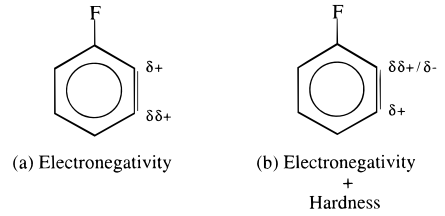

Figure 6. Polarization of the σ bond in 3-fluorobenzyne due to the influence of electronegativity of fluorine (a) and the combined influence of electronegativity and hardness (b) of fluorine.

C_2, decrease ($C_1 < C_2$) in both cases (3- and 4-fluorobenzyne) with the distance to the F atom. This is not what one would expect using only the electronegativity χ of the F atom ($\chi_F = 10.41$ and $\chi_C = 6.27$[13]), as is shown in Figure 6a.

However in previous studies it was found that in the absence of resonance the role of the hardness of a substituent can be very important.[23] Hardness is considered to be a measure of the resistance of a system to a change in the number of electrons, thus related to the inverse of the charge capacity of the system. As this effect is opposite of the effect of the electronegativity, a competition between these two driving forces can be expected[23] (cf. Figure 6b). In fluorine the electronegativity and the hardness ($\eta_F = 7.01$ and $\eta_C = 5.0$[13]) are known to be very large, the resulting effect being dependent on the system it is introduced in. The higher the softness (polarizability) of the host system, the smaller the effect of the hardness of the substituent.[23i,m,41] Furthermore the hardness is an effect of the substituent itself, even though the introduction of a hard substituent in a system is known to increase the global hardness of the system; the hardness of the isolated substituent mainly describes the local behavior of the substituent in the system. This will become clear when discussing Figure 7, schematically depicting the changes in electron populations at the different atoms as a function of the distance to F. C_3 or both C_3 and C_4, in the case of 3-fluorobenzyne and 4-fluorobenzyne, respectively, are situated between F and C_2 on the horizontal axis.

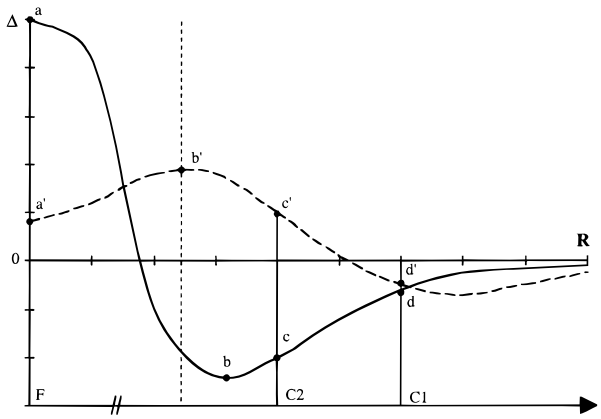

Figure 7. Electronic populations on the different atoms in the fluorobenzynes as a function of the distance to fluorine. Differences with respect to the isolated atoms Δ are given as a function of the distance to the fluorine atom.

Considering only the electronegativity (neglecting hardness), the following points can be made.

Point a: The number of electrons at F will increase as compared to the isolated atom as electrons are drawn from the rest of the system toward F. This increase is substantial as the electronegativity is large.

Point b: The electronegativity has the largest effect on atoms close to the substituent (C_3 in 3-fluorobenzynes, C_4 in 4-fluorobenzyne). The decrease in the number of electrons will be maximum.

Points c and d: The number of electrons increases from c to d due to the decrease of the effect of electronegativity with the distance from the substituent. As atoms C_2 and C_1 are in this region, the population on C_1 is larger.

Considering both electronegativity and hardness, the following points can be made.

Point a′: The number of electrons at F will increase as electrons are drawn from the rest of the system toward F. This

TABLE 4: Calculated Fukui Functions Using NPA Electron Populations (in au) for 3-Fluorobenzyne and 4-Fluorobenzyne at the Four DFT Levels with the cc-pVDZ and cc-pVTZ Basis Sets.

system	level	basis set	$f^+_{C_1}$(tot)	$f^+_{C_2}$(tot)	$f^+_{C_1}(\pi)$	$f^+_{C_2}(\pi)$	$f^+_{C_1}(\sigma)$	$f^+_{C_2}(\sigma)$	$f^+_{C_1}$(tot) − $f^+_{C_2}$(tot)
4-fluorobenzyne	SVWN	cc-pVDZ	0.284 71	0.281 43	−0.089 25	−0.086 04	0.373 96	0.367 47	0.006 49
	BLYP		0.277 73	0.275 15	−0.091 75	−0.088 40	0.36 948	0.363 55	0.005 93
	B3LYP		0.283 41	0.284 21	−0.094 08	−0.089 38	0.377 49	0.373 59	0.003 90
	B3PW91		0.284 45	0.286 72	−0.091 90	−0.088 49	0.376 35	0.375 21	0.001 14
	SVWN	cc-pVTZ	0.286 49	0.281 75	−0.082 52	−0.081 07	0.369 01	0.362 82	0.006 19
	BLYP		0.279 79	0.275 86	−0.085 32	−0.083 08	0.365 11	0.358 94	0.006 17
	B3LYP		0.288 23	0.282 13	−0.087 02	−0.084 83	0.375 25	0.366 96	0.008 29
	B3PW91		0.287 65	0.284 83	−0.085 17	−0.084 06	0.372 82	0.368 89	0.003 93
3-fluorobenzyne	SVWN	cc-pVDZ	0.295 06	0.270 19	−0.090 55	−0.071 54	0.385 61	0.341 73	0.043 88
	BLYP		0.286 02	0.268 35	−0.095 57	−0.074 25	0.381 59	0.342 60	0.038 99
	B3LYP		0.296 47	0.274 25	−0.098 51	−0.074 15	0.394 98	0.348 40	0.046 58
	B3PW91		0.295 80	0.277 69	−0.095 35	−0.073 45	0.391 15	0.351 14	0.040 01
	SVWN	cc-pVTZ	0.302 26	0.263 19	−0.084 77	−0.068 08	0.387 03	0.331 27	0.055 76
	BLYP		0.293 67	0.262 64	−0.089 74	−0.070 89	0.383 41	0.333 53	0.049 88
	B3LYP		0.305 1 0	0.264 98	−0.092 88	−0.071 00	0.397 98	0.335 98	0.062 00
	B3PW91		0.302 79	0.268 68	−0.090 22	−0.070 02	0.393 01	0.338 70	0.054 31

increase is however much lower than in the case where the hardness was neglected, as the hardness, related to the inverse of the charge capacity,[42] of F prohibits the accommodation of additional electrons on the F atom.

Point b′: As the hardness primarily has a local effect and the neighboring atoms have a larger charge capacity, an increase in population can be observed on the nearest neighbor(s). Due to the competition between electronegativity and hardness, the curve has the same shape, even though the changes in electron densities are less pronounced, as the one obtained when neglecting hardness but seems to be shifted away from the F atom (point b′ in this curve corresponds to the point a in the curve describing the effect of the electronegativity neglecting the hardness).

Points c′ and d′: The atoms of the triple bond, C_2 and C_1, will now be in the area where the number of electrons decreases with respect to the distance from the substituent. This leads to a larger population on C_2 than on C_1.

In the case of the hetaryne we have a completely different story. The π-mesomeric effect is in this case of inferior importance, as it will not give rise to any polarization of the triple bond. On the other hand the selectivity of a nucleophilic attack for C_1 can easily be explained in terms of the σ-mesomeric effect, in which the third bond of the triple bond is involved together with the free electron pair of nitrogen, which is also located in a sp^2 orbital. The relevant mesomeric form is shown in Figure 4. This is confirmed by the σ-electron populations on C_1 and C_2. The inductive effect is also present in this system but will be, as is generally excepted, much smaller than the mesomeric one.

The fact that inductive effects are much smaller than mesomeric effects also gives us the means to explain the regioselectivity sequence given in Figure 2. Whereas the difference in regioselectivity in the fluorobenzynes is attributed to an inductive effect (electronegativity modulated by hardness) which decreases with the distance to the substituent, the much larger selectivity in the case of the hetaryne can be attributed to the σ-mesomeric effect involved in the polarization of the triple bond. Again this is confirmed by the σ-electron populations on C_1 and C_2. Here we see that the difference in the poplation on C_1 and C_2 increases, indicating an increase in the polarization of the relevant bond.

As mentioned in the Introduction, the reactivity of the hetaryne was already investigated with success using the Fukui function f^+. Here the Fukui function was found to give a correct description of the intramolecular reactivity sequence. This result was confirmed at the DFT level by means of a B3LYP/cc-pVDZ calculation ($f^+_{C_4}$(tot) = 0.019 02 and $f^+_{C_5}$(tot) = −0.087 36). The same study at the HF/3-21G level showed the Fukui function to fail as a reactivity descriptor[43] for the substituted benzynes. The results of the calculation of f^+ at different DFT levels for these systems will now be discussed. On the basis of the success of the use of σ and π populations in the previous part, the condensed Fukui function using the total NPA population and its σ and π components (see Table 4) was chosen. When studying these results, it becomes immediately clear that the total Fukui function f^+_C(tot) gives a correct description of the regioselectivity in 3-fluorobenzyne at all DFT levels using both basis sets. One does observe a significant decrease in the difference between $f^+_{C_1}$(tot) and $f^+_{C_2}$(tot) when going from the cc-pVTZ basis to the less extended cc-pVDZ basis. In the case of 4-fluorobenzyne this behavior even leads to an inversion of the regioselectivity according to the f^+_C(tot) for B3LYP/cc-pVDZ and B3PW91/cc-pVDZ calculations.

Considering the σ and π compounds of the condensed Fukui function, $f^+_C(\sigma)$ and $f^+_C(\pi)$, it immediately becomes clear that the nucleophilic attack will take place in the σ plane (positive values for $f^+_C(\sigma)$) and not perpendicular to this plane (negative values for $f^+_C(\pi)$). Furthermore the $f^+_C(\sigma)$ is found to predict a reaction at C_1 in all cases, again in agreement with experiment. Finally the increase in regioselectivity when going from 4-fluorobenzyne to 3-fluorobenzyne is also described correctly as the difference $f^+_{C_1}(\sigma) - f^+_{C_2}(\sigma)$ increases (see Table 4).

4. Conclusions

The geometry and reactivity of four intermediates of the benzyne and hetaryne type were studied using both ab initio and DFT methods. The DFT methods are able to describe the (electronic) structure of these systems with accuracies comparable to traditional correlated molecular orbital methods at a decreased computational cost. Furthermore these techniques are observed to assign more triple-bond character to the CC bond in the ring plane on which the nucleophilic addition occurs.

In the reactivity study the Fukui function was found to be an adequate descriptor of the regioselectivity in accordance with (among others, our) previous findings on a diversity of structures. The influence of the fluorine substituent turned out to be again a combination of opposing electronegativity and hardness effects, as demonstrated in the charge distribution of the parent reactive intermediate.

The whole of this study illustrates the capability of present day DFT methods to study both structural and reactivity aspects of reactive intermediates.

Acknowledgment. W.L. and F.D.P. are indebted to the Fund for Scientific Research-Flanders (Belgium) (FWO) for their position as postdoctoral fellow ("Postdoctoraal Onderzoeker"). P.G. wishes to thank the Free University of Brussels for a generous computer grant and the FWO for continuous support.

References and Notes

(1) Carey, F.; Sundberg, R. *Advanced Organic Chemistry*, 3rd ed. part A; Plenum Press: New York−London, 1990; p 221.
(2) See ref 1, part B, p 588.
(3) Miller, J. In *Aromatic Nucleophilic Substitution* in *Reaction Mechanisms in Organic Chemistry*; Eaborn, C., Chapman, N. B., Ed.; Elsevier: Amsterdam−London−New York, 1968.
(4) March, J. *Advanced Organic Chemistry*, 3rd ed.; John Wiley: New York, 1985; p 580.
(5) Møller, C.; Plesset, M. S. *Phys. Rev.* **1934**, *46*, 618.
(6) Szabo, A.; Ostlund, N. S. *Modern Quantum Chemistry*; Macmillan Publishing Co.: New York, 1982; Chapter 4.
(7) Hunt, W. J.; Hay, P. J.; Goddard, W. A., III. *J. Chem. Phys.* **1972**, *57*, 738.
(8) Bobrowicz, F. W.; Goddard, W. A., III. *Modern Theoretical Chemistry*; Schaefer, H. F., Plenum: New York, 1977; Vol. 3, p 79.
(9) Bartlett, R. J. *J. Phys. Chem.* **1989**, *93*, 1697.
(10) Wahl, A. C.; Das, G. *Modern Theoretical Chemistry*; Schaefer, H. F., III, Ed.; Plenum: New York, 1977; Vol. 3, p 51.
(11) Martin, J. M. L.; François, J. P.; Gijbels, R. *Chem. Phys. Lett.* **1990,** *172*, 346.
(12) Langenaeker, W.; De Proft, F.; Geerlings, P. *J. Mol. Struct. (THEOCHEM)* **1994** *313*, 283.
(13) Parr, R. G.; Yang, W. *Density Functional Theory of Atoms and Molecules*; Oxford University Press: New York, 1989.
(14) Hohenberg, P.; Kohn, W. *Phys. Rev. B* **1964**, *136*, 864.
(15) Kohn, W.; Sham, L. J. *Phys. Rev.* **1965**, *140*, 1133.
(16) See for example: (a) White, C. A.; Johnson, B. G.; Gill, P. M. W.; Head-Gordon, M. *Chem. Phys. Lett.* **1996**, *253*, 268. (b) Burant, J. C.; Scuseria, G. E.; Frisch, M. J. *J. Chem. Phys.* **1996**, *105*, 8969.
(17) Tielemans, M.; Aresckha, V.; Colomer, J.; Promel, R.; Langenaeker, W.; Geerlings, P. *Tetrahedron* **1992**, *48*, 10575.
(18) Hoffmann, R. W. *Dehydrobenzenes and Cycloalkynes*; Academic Press: New York, 1967.
(19) Bonaccorsi, R.; Scrocco, E.; Tomasi, J. *J. Chem. Phys.* **1970**, *52*, 5270.
(20) Pearson, R. G. *J. Am. Chem. Soc.* **1963**, *85*, 3533.
(21) Parr, R. G.; Yang, W. *J. Am. Chem. Soc.* **1984**, *106*, 4049.
(22) For a recent review, see for example: Parr, R. G.; Yang, W. *Annu. Rev. Phys. Chem.* **1995,** *46*, 701.
(23) (a) Langenaeker, W.; Demel, K.; Geerlings, P. *J. Mol. Struct. (THEOCHEM)* **1991**, *234*, 329. (b) Langenaeker, W.; Demel, K.; Geerlings, P., *J. Mol. Struct. (THEOCHEM)* **1992**, *259*, 317. (c) Baeten, A.; De Proft, F.; Langenaeker, W.; Geerlings, P. *J. Mol. Struct. (THEOCHEM)* **1994**, *306*, 203. (d) Langenaeker, W.; Coussement, N.; De Proft, F.; Geerlings, P. *J. Phys. Chem.* **1994**, *98*, 3010. (e) De Proft, F.; Choho, K.; Amira, S.; Geerlings, P. *J. Phys. Chem.* **1994**, *98*, 5227. (f) Langenaeker, W.; De Proft, F.; Geerlings, P. *J. Phys. Chem.* **1995**, *99*, 6424. (g) De Proft, F.; Langenaeker, W.; Geerlings, P. *Int. J. Quantum Chem.* **1995**, *55*, 459. (h) De Proft, F.; Langenaeker, W.; Geerlings, P. *Tetrahedron* **1995**, *51*, 4021. (i) Damoun, S.; Langenaeker, W.; Van de Woude, W.; Geerlings, P. *J. Phys. Chem.* **1995**, *99*, 12151. (j) Geerlings, P.; De Proft, F.; Langenaeker, W. in *Density Functional Methods: Applications in Chemistry and Materials Science*; Springborg, M., Ed.; John Wiley: New York, Chapter 2, 1997. (k) Geerlings, P.; Langenaeker, W.; De Proft, F.; Baeten, A. In *Molecular Electrostatic Potentials−Concepts and Applications*; Murray, J. S., Sen, K. D., Eds.; Elsevier: Amsterdam, 1996; pp. 587−617. (l) Damoun, S.; Langenaeker, W.; Geerlings, P. *J. Phys. Chem. A* **1997**, *101* (36), 6951. (m) Geerlings, P.; De Proft, F.; Langenaeker, W. *Adv. Quantum Chem.*, in press.
(24) Sanderson, R. T. *Polar Covalence*; Academic Press: New York, 1983.
(25) Yang, W.; Parr, R. G. *Proc. Natl. Acad. Sci. U.S.A.* **1985,** *82*, 6723.
(26) Parr, R. G.; Pearson, R. G. *J. Am. Chem. Soc.* **1983**, *105*, 7512.
(27) Parr, R. G.; Donnely, R. A.; Levy, M.; Palke, W. E. *J. Chem. Phys.* **1978**, *68*, 3801.
(28) Yang W.; Mortier W. J. *J. Am. Chem. Soc.* **1986**, *108*, 5708.
(29) Dirac, P. A. M. *Cambridge Philos. Soc.* **1930**, *26*, 376.
(30) Vosko, S. H.; Wilk, L.; Nusair, M. *Can. J. Phys.* **1980**, *58*, 1200.
(31) Becke, A. D. *Phys. Rev. A* **1988**, *38*, 3098.
(32) Lee, C.; Yang, W.; Parr, R. G. *Phys. Rev. B* **1988**, *37*, 785.
(33) Becke, A. D. *J. Chem. Phys.* **1993,** *98*, 5648.
(34) Frisch, M. J.; Trucks, G. W.; Schlegel, H. B.; Gill, P. M. W.; Johnson, B. G.; Robb, M. A.; Cheeseman, J. R.; Keith, T.; Petersson, G. A.; Montgomery, J. A.; Raghavachari, K.; Al-Laham, M. A.; Zakrzewski, V. G.; Ortiz, J. V.; Foresman, J. B.; Cioslowski, J.; Stefanov, B. B.; Nanayakkara, A.; Challacombe, M.; Peng, C. Y.; Ayala, P. Y.; Chen, W. Wong, M. W.; Andres,. J. L; Replogle, E. S.; Gomperts, R.; Martin, R. L.; Fox, D. J.; Binkley, J. S.; Defrees, D. J.; Baker, J.; Stewart, J. P.; Head-Gordon, M.; Gonzalez, C.; Pople, J. A. *Gaussian 94, Revision C.3*; Gaussian, Inc.: Pittsburgh, PA, 1995.
(35) Dunning, T. H., Jr. *J. Chem. Phys.* **1989**, *90*, 1007.
(36) (a) De Proft, F.; Geerlings, P. *J. Chem. Phys.* **1997**, *106*, 3270. (b) Geerlings, P.; De Proft, F.; Martin, J. M. L. In *Recent Developments in Density Functional Theory*; Seminario, J., Ed.; Elsevier: Amsterdam, 1996; pp 773−809. (c) De Proft, F.; Martin, J. M. L.; Geerlings, P. *Chem. Phys. Lett.* **1996**, *256*, 400. (d) De Proft, F.; Martin, J. M. L.; Geerlings, P. *Chem. Phys. Lett.* **1996**, *250*, 393.
(37) Pople, J. A.; Head-Gordon, M.; Raghavachari, K. *J. Chem. Phys.* **1987**, *87*, 5968.
(38) Reed, A. E.; Curtiss, L. A.; Weinhold, F. *Chem. Rev.* **1988**, *88*, 899.
(39) Van Lier, G.; De Proft, F.; Geerlings, P. *Chem. Phys. Lett.* **1997**, *274*, 396.
(40) (a) Radom, L.; Nobes, R. H.; Underwood, D. J.; Wai-Kee, L. *Pure Appl. Chem.* **1986**, *58*, 75. (b) Rigby, K.; Hillier, I. H.; Vincent, M. A., *J. Chem. Soc., Perkin Trans. 2* **1987**, 117. (c) Hillier, I. H.; Vincent, M. A.; Guest, M. F.; Von Niessen, W. *Chem. Phys. Lett.* **1987**, *134*, 403. (d) Scheiner, A. C.; Schaefer, H. F., III; Liu, B. *J. Am. Chem. Soc.* **1989**, *111*, 3118. (e) Scheiner, A. C.; Schaefer, H. F., III. *Chem. Phys. Lett.* **1991**, *177*, 471. (f) Liu, R.; Xuenfeng, Z.; Pulay, P. *J. Phys. Chem.* **1992**, *96*, 259. (g) Sutter, H. U.; Ha, T.-K. *Chem. Phys. Lett.* **1992**, *198*, 259. (h) Nicolaides, A.; Borden, W. T. *J. Am. Chem. Soc.* **1993**, *115*, 11951. (i) Wiershke, S. G.; Nash, J. J.; Squires, R. R., *J. Am. Chem. Soc.* **1993**, *115*, 11958. (j) Karadahov, P. B.; Gerrat, J.; Raos, G.; Cooper, D. L.; Raimondi, M. *Isr. J. Chem.* **1993**, *33*, 253. (k) Kraka, E.; Cremer, D. *Chem. Phys. Lett.* **1993**, *216*, 333. (l) Kraka, E.; Cremer, D. *J. Am. Chem. Soc.* **1994**, *116*, 4936. (m) Lindh, R.; Persson, B. J. *J. Am. Chem. Soc.* **1994**, *116*, 4963. (n) Lindh, R.; Lee, T. J.; Bernhardsson, A.; Persson, B. J.; Karlström, G. *J. Am. Chem. Soc.* **1995**, *117*, 7186. (o) Nash, J. J.; Squires, R. R. *J. Am. Chem. Soc.* **1996**, *118*, 11872. (p) Kraka, E.; Cremer, D.; Bucher, G.; Wandel, H.; Sander, W. *Chem. Phys. Lett.* **1997**, *268*, 313.
(41) Langenaeker, W.; Tielens, F.; Geerlings, P. In preparation.
(42) Politzer, P.; Murray, J. S.; Grice, M. E. In *Chemical Hardness*; Sen, K. D., Ed.; Springer-Verlag: Berlin−Heidelberg, 1993; p 101.
(43) Langenaeker, W.; Geerlings, P. Unpublished results.